ISSN 1330–0008
CODEN FIZAE4

AN ELECTRON MICROSCOPY STUDY OF THE "CHAIN"–LAYER ORDERING IN THE YBCO-TYPE HIGH–T_c SUPERCONDUCTORS

OGNJEN MILAT

Institute of Physics of the University, Bijenička 46; POBox 304; HR-10001 Zagreb, Croatia

Dedicated to Professor Mladen Paić on the occasion of his 90$^{\mathrm{th}}$ birthday

Received 23 June 1995

UDC 538.945

PACS 61.10.-i, 61.14.-x, 74.72.-h

Structures of a number of high-T_c superconducting cuprates related to the prototype YBCO compound, were studied by means of high resolution electron microscopy (HREM) and electron diffraction (ED). Commensurate superstructures or incommensurate modulated structures were induced by various metal atom substitutions for Cu in the "chain"-layer and its ordering. Metal (M) and oxygen (O) atom ordering is confined mainly in the MO_{1-x}-"chain" layers, while the remaining part of the crystal structure, as well as the material's superconducting features, are hardly affected.

1. Introduction

The basic crystal structure of the high-T_c superconducting cuprates is related with the perovskite ABO_3 lattice (a_p = 0.38 nm). The crystal structure of $YBa_2Cu_3O_{7-x}$ (usually called YBCO) consists of three perovskite units, some of them being oxygen deficient. The layered structures of all superconducting cuprates are characterized by at least one CuO_2 two–dimensional layer, which is generally believed to be crucial for superconductivity. The structure of YBCO is additionally characterized by the so-called "chain"–layer [1], i.e. the oxygen deficient layer with the composition MO_{1-x} (M = metal or metalloid atom). In pure YBCO (which is also referred as "123" or Cu-1212 phase [2], where M = Cu and $x = 0$), the Cu and O atoms are arranged in a configuration of "chains" which run along one of the principal lattice directions, and which is in fact responsible for the orthorhombic crystal structure of the lattice cell: $a_0 \geq a_p^{(1)}$; $b_0 \leq a_p^{(2)}$; $c_0 \approx 3a_p^{(3)}$.

Since the discovery of high-T_c superconductivity of (LBCO) in 1986 [3] and YBCO in 1987 [4], a large number of YBCO-derivative compounds were synthesized by doping or by substitution of isovalent (or oliovalent) ions in the prototype YBCO material [5]. It was found that O atom can be partially substituted by a vacancy, or F, or Cl atoms [6]; that Ba can be substituted by Sr, or Ln elements; Y by Ca, or Ln (rare earth) [7]; Cu atoms can be selectively replaced by various metals: Ni, Ta, Ga, Co, Al, Hg, ... [8-10], or even by the anion complexes such as SO_4, PO_4, or CO_3 [6].

In this paper the results of an extended electron microscopy study of YBCO related compounds will be presented. These results show that partial or complete substitutions of Cu atoms by Ga, Al, Hg, or S atoms in the "chain"-layer induce commensurate superstructures [11-19] or incommensurate modulated structures [20] without profound changes of the basic structural features [11].

2. *Disordering of "chains" by partial* Cu *substitution in the* M/Cu-*1212 compounds*

When various metallic elements (M = Fe, Zn, Ta, Nb, Co, Ga, ...) are substituted for Cu at low level (< 5%) in the $YBa_2(Cu_{1-x}M_x)_3O_7$ compound, the microstructural changes were evidenced as fragmentation of twin domains and reduction of their sizes [12]. The orthorhombic spot splitting in the electron–difraction

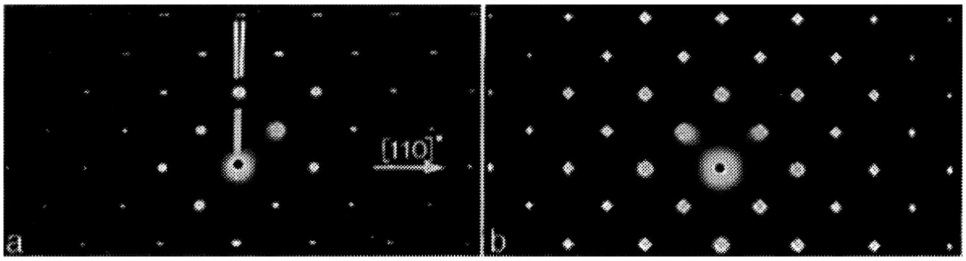

Fig. 1. The [001] *zone electron diffraction pattern of undoped* YBCO*–(a), and 5%* Fe *doped* YBCO*–(b).*

(ED) pattern (shown in Fig. 1a), which is characteristic of pure YBCO, becomes less pronounced in the doped YBCO, eventually being exchanged by the pattern of streaked spots with pseudo tetragonal symmetry (see Fig. 1b). This is due to frequent changing of the CuO–"chain" orientation at each doped atom as a point defect; the "chain" direction which is associated with the orthorhombic b_0 axis (Fig. 2a), changes locally here and there from $b_0 = [010]_p$ to $b_0 = [100]_p$, and vice versa, so that no single domain can be created. The resulting "tweed structure" is usually accompanied by a decrease in T_c [12].

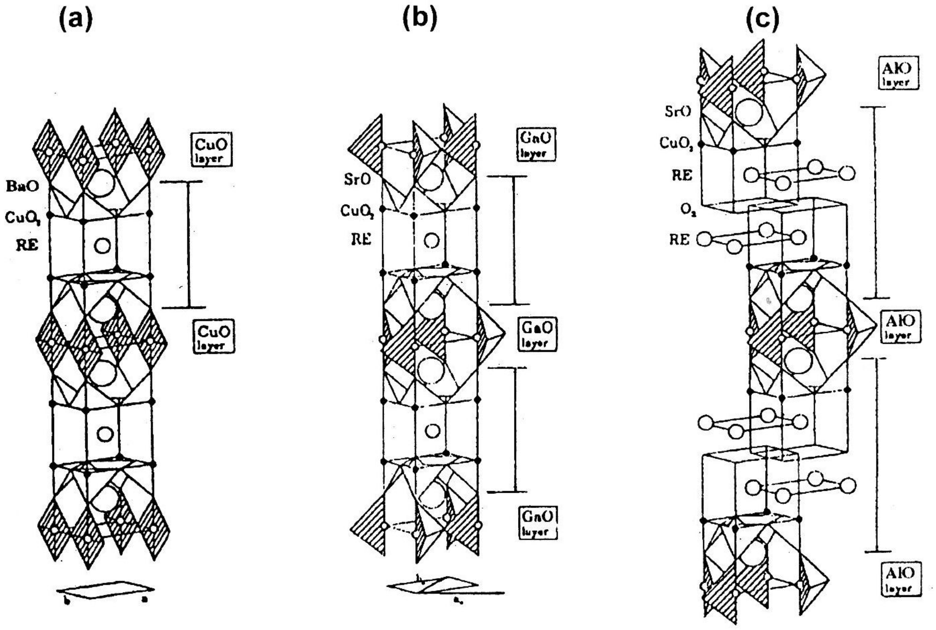

Fig. 2. Schematic representation of basic unit cells of: (a) $YBa_2Cu_3O_7$ *(*Cu-*1212 phase); (b)* $RESr_2GaCu_2O_7$ *(*Ga-*1212 phase);* $(RE)_2Sr_2AlCu_2O_9$ *(*Al-*1222 phase).*

3. Superstructures in the M-*1212 compounds* (M = Ga, Al, Hg, S)

3.1. Diagonally running "chains" in the Ga–*1212 phase*

Complete substitution of Ga for Cu in the "chain"–layers of the YBCO can be achieved in the $(Nd_{0.75}Ce_{0.25})Sr_2GaCu_2O_7$ compound if simultaneous replacement of Sr for Ba takes place in the adjacent layers [13] above and below the "chain"–layer (see Fig. 2). While the replacement of Sr for Ba atom, constituting the (Ba/Sr)O layers which are of the RS-structure type, and of Nd/Ce for Y, constituting the F-type layer [1], do not change the topology of the overall crystal structure, the substitution by Ga for Cu strongly affects its symmetry [14]. Namely, due to strong tendency of the Ga atoms to be tetrahedrally coordinated by the surrounding oxygen atoms in the form of GaO_4 tetrahedra (Fig. 2b), the GaO layers adopt a configuration of corner–sharing tetrahedra "chains", which now run along the diagonal perovskite $[110]_p$ direction [14]. This highly contrasts the "chains" of the corner sharing CuO_4 square planar units running along the principal $[010]_p$ direction in pure YBCO, (Fig. 2a). These structural features were revealed by the high–resolution–electron–microscopy (HREM) imaging of the Ga-1212 structure shown in Fig. 3. Horizontal rows of the separated bright dots in Fig. 3 represent the Y-layers, as it is indicated in the legend. The rows of dark horizontal bars associated with the pair of dark dots in the right part of Fig. 3 (marked by open circles at the vertices of the rectangle representing superlattice unit cell), indicate the GaO layers, where the GaO_4 "chains" run edge–on along the imaging direction, i.e, along the $[110]_p$ axis. The horizontal rows of dark dot pairs turn to the rows of equally separated dark dots in the left part of Fig. 3, representing the GaO layers where the GaO_4 tetrahedra "chains" run perpendicular to the imaging direction, i.e., along the $[-110]_p$ axis of basic crystal lattice [14,15]. Two insets in Fig. 3 reveal the differences in the corresponding ED patterns. The additional weak spots in the right inset, which are situated in the centres of rectangular mesh of the basic spots, are due to the staggering configuration of the "chains" in successive GaO layers. No such spots are present besides the basic ones in the left inset, in agreement with the fact that no staggering can be observed by imaging perpendicular to the "chains". Moreover, the superlattice spot extinction along this zone perpendicular to the "chains" indicate the symmetry relation (glide mirror plane) between the pairs of tetrahedra forming each "chain" [14,16]. The diagonally running GaO_4 tetrahedra "chain" superlattice cell in the GaO layer is schematically represented in Fig. 4a.

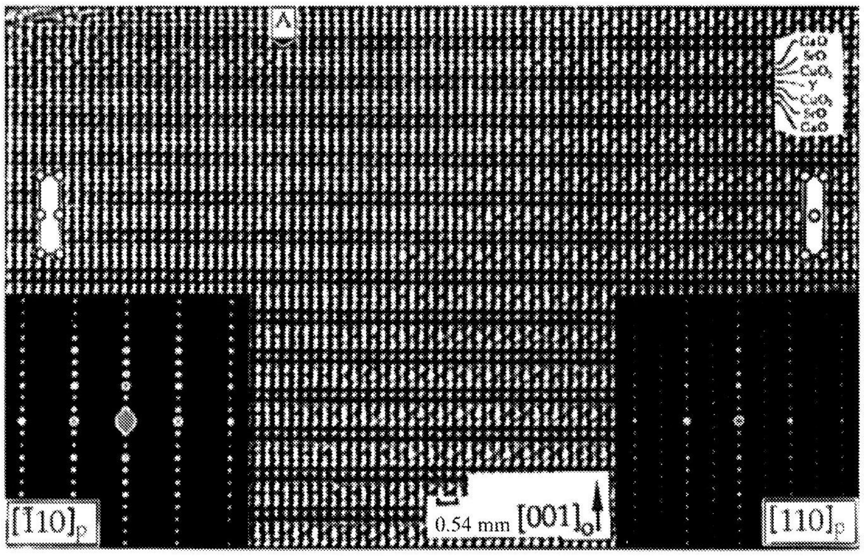

Fig. 3. High resolution imaging of the Ga*-1212 structure along the* $[110]_p$ *direction; the diagonal "chains" in* GaO *layers run in the right part – along, in the left part perpendicular to the imaging direction. Insets represent corresponding electron diffraction patterns.*

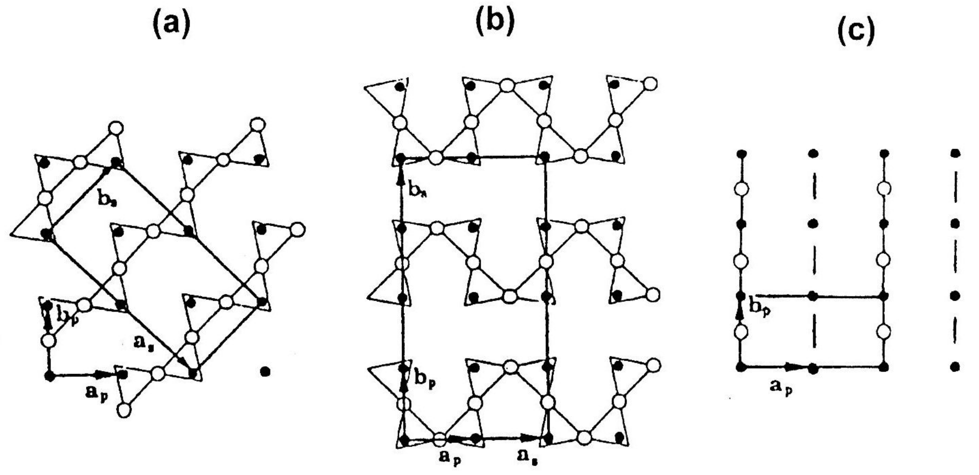

Fig. 4. Schematics of the two–dimensional "chain" arrangements on the superlattice unit cells in the MO *layers: (a) diagonal* GaO_4*-chains along the* $[110]_p$ *direction in the* Ga-*1212 phase; (b) meandering* AlO_4*-chains along the* $[100]_p$ *direction in the* Al-*1222 phase; alternating chains along the* $[010]_p$ *direction in the* (Hg/Pr)-*1212 phase.*

3.2. Meandering "chains" in the Al-*1222 phase*

In the Al-1222 compound $(Y_{0.90}Ce_{0.10})_2(Sr_{0.85}Ce_{0.15})_2AlCu_2O_9$ the complete substitution of Al for Cu in the "chain" layers is accompanied by the Sr/Ce for Ba replacement in the adjacent RS-type layers, and besides that, the single Y layer is substituted by the Ce doped (Y/Ce)-O_2-(Y/Ce) lamella [17] with the F-type layer structure [1], (Fig. 2c). As Al atom has also a strong tendency to be tetrahedrally coordinated by O atoms like a Ga atom, an ordering takes place in the AlO layers of the Al-1222 structure in the form of "chains" of corner sharing AlO_4 tetrahedra [17]. However, the interpretation of HREM imaging and ED pattern, shown in Fig. 5 disclosed a configuration of meandering "chains", which turns out to be quite different in comparison to the diagonal "chain" arrangement in the Ga-1222 structure [14]. In Fig. 5a, which was taken close to the thin edge of the wedge-shaped crystal, all relevant features of the basic Al-1222 structure are revealed, however, with no discernible feature indicating the "chain" superlattice. On the other hand, the AlO_4 "chain" superlattice is clearly represented only in the imaging of the thicker region of the same wedge–shaped crystal (Fig. 5b). The imaging conditions for the thin crystal (Fig. 5a) where such that the bright dots represent the channels between atomic columns, while the dark dots point to the projections of metal atoms [17]. The horizontal rows of bright and dark dots thus correspond to the constituting layers as indicated in the legend of Fig. 5a, while the brightest dots in Fig. 5b reveal the channels between the AlO_4 tetrahedral "chains". Separation between these dots is $2a_p$, in agreement with the spacing between the successive meandering "chains" in each AlO layer [17]. This meandering "chain" configuration, an the corresponding superlattice unit cell in the AlO layer, are schematically shown in Fig. 4b. The ED patterns along the $[100]_p$, and $[120]_p$ zones shown in Figs. 5c and d, respectively, contain streaks of weak spots; the superlattice spot extinctions and their positions with respect to the basic spots reveal the symmetry of the meandering "chain" superlattice [17].

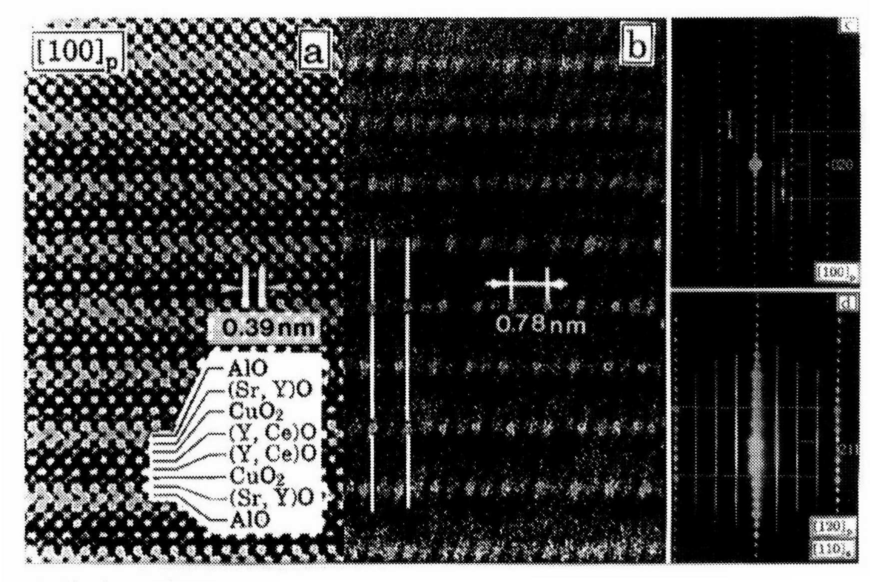

Fig. 5. High resolution imaging of the Al-*1222 structure along the* $[010]_p$ *zone: (a) small thickness; (b) larger thickness; Electron diffraction patterns along: (c)* $[100]_p$ *zone; (d)* $[120]_p$ *zone.*

3.3. Alternating "chains" on a $2a_p \times a_p \times c_p$ superlattice in the (Hg/Pr)-1212 phase

Mercury atom in the Hg-1212 compound can be partially substituted by Pr atom in the $(Ca/Pr)Sr_2(Hg_{0.5}Pr_{0.5})Cu_2O_{6+x}$ compound inducing the $2a_p \times a_p \times c_p$ superlattice [18]. The HREM imaging along the $[010]_p$ zone, shown in Fig. 6a, reveals horizontal rows of dots with two times larger periodicity then the remaining bright–dot rows which represent the layers of the basic structure; the corresponding ED patterns are shown in Figs. 6b and c. The rows marked in Fig. 6a were identified to be the "chain" layers [18], while the double periodicity can be interpreted in the following way: the Hg-"chains", which run along the imaging $[010]_p$ direction alternate regularly with the Pr-"chains" along the $a_p = [100]_p$ direction, in each (Hg/Pr)O layer. As marked by large dots in Fig. 6a, and revealed by the positions of the superlattice spots in the ED patterns in Figs. 6b and c, the stacking of successive layers can stagger, or coincide vertically. A schematic representation of alternating "chains" on the superlattice unit cell in the (Hg/Pr)O layer is shown in Fig. 4c.

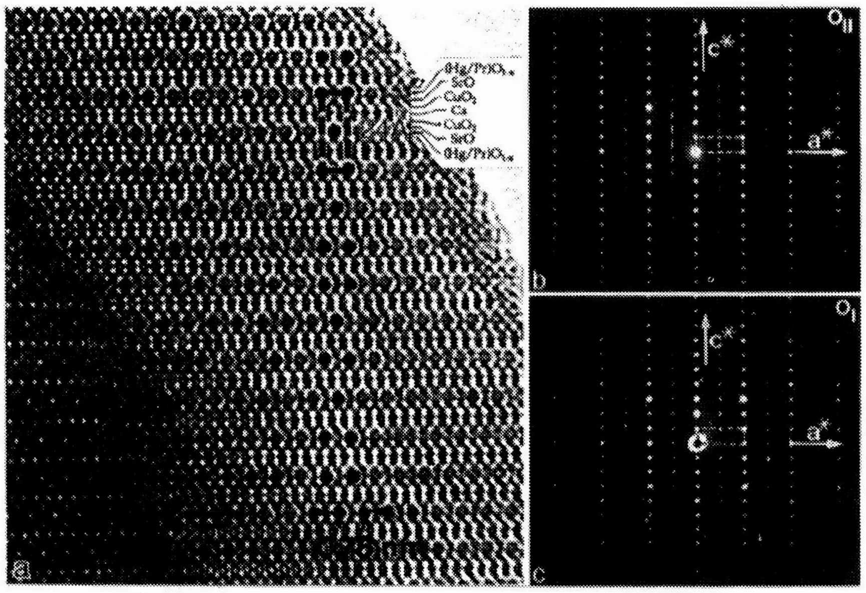

Fig. 6. High resolution imaging of the (Hg/Pr)-*1212 structure along* $[010]_p$ *direction–(a); Electron diffraction patterns along the* $[010]_p$ *zones revealing stagger–(b), and vertical–(c) stacking of* Hg-*"chains".*

3.4. Concentration "chains" in the modulated structure of the S/Cu-*1212 phase*

Cu atoms in the "chain" layers can be partially substituted by S atoms in the S/Cu-1212 compound: $(Y/Ca/Sr)Sr_2(Cu_{0.8}(SO_4)_{0.2})Cu_2O_{6.2-x}$ [6]. The SO_4 units are more compact than the MO_4 tetrahedra (with M = Ga, Al, ...) and they were expected to replace CuO_4 square planar units (of pure YBCO) with no mutual interaction between them [19]. However, the configurations of linear clusters of SO_4 tetrahedra in the form of "chain" waves along an oblique direction [20] can be observed in the HREM imaging (Fig. 7). The basic structure, as well as an incommensurate modulated structure, is clearly revealed in Fig. 7a; horizontal rows of bright and dark dots correspond to the layers indicated in the legend. The clusters of four brightest dots, marked by the crosses in the upper–right part of Fig. 7a, can be associated with the positions of the SO_4 "chains" imaged edge–on. Due to only partial S for Cu substitution and to the fractional stoichiometry in the "chain" layer, S/Cu = 0.22/0.78, the "chains" are incommensurably ordered with respect to the underlying basic structure; the sequences of two to three CuO-"chains" (running along the $b_0 = [010]_p$ axis) are succeeded by the SO-"chain" along the principal $a_0 = [100]_p$ axis in each (Cu/S)O layer. The average spacing between the S-concentration "chains" was found to be the harmonic mean of the $4a_p$ and $3a_p$ [20], i.e, the modulation period $a_m = 3.43a_p$ is incommensurate with respect to the basic lattice periodicity. The S-"chains" in successive layers are stacked in such a way that the modulation wave vector in reciprocal space encloses an angle of 29° with the $[h00]_p^*$ row of spots in ED pattern of Fig. 7b. The interpretation of this incommensurate modulated structure in terms of SO_4-"chain" concentration waves [20] is indicated in Fig. 7a by the two families of parallel lines which cross close to the highest SO_4-"chain" concentration. The incommensurate features of this modulated structure, as imaged in Fig. 7a, are in complete agreement with the ED patterns along the $[010]_p$, and $[001]_p$ zones, shown in Figs. 7b and c, respectively.

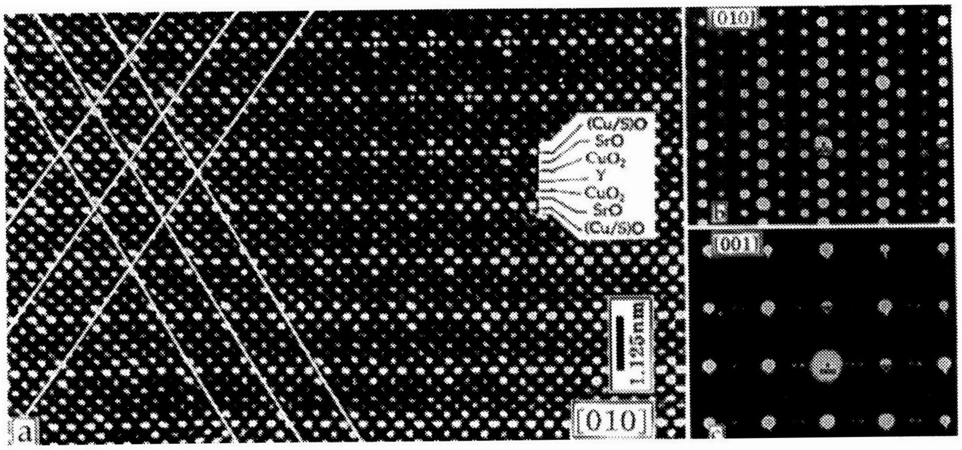

Fig. 7. High resolution imaging of the S/Cu-*1212 structure along the* $[010]_p$ *direction–(a); Electron diffraction pattern along the* $[010]_p$*–(b), and the* $[001]_p$*–(c) zone.*

4. Discussion

The "chain" ordering in the MO_{1-x} layers presented so far for the M-1212 compounds with M = Ga, Al, Hg, S, has to be distinguished from the oxygen or oxygen–vacancy ordering in the $YBa_2Cu_3O_{7-x}$ compound [21,22]. Namely, the vacancy ordering in the so-called OrthoII and OrthoIII superstructure with $x = 0.5$, and $x = 0.66$, (where each CuO "chain" is succeeded by one (or two) Cu-vacancy row(s) in each CuO_{1-x} layer) strongly affects superconducting properties (reduces T_c to 0 K for $x \geq 0.66$ [21,22]). On the other hand, the "chain"–layer ordering presented here for a number of M-1212 compounds does not "kill" superconductivity although T_c, as well as the oxygen stoichiometry, can be slightly affected [6].

5. *Conclusions*

Electron microscopy and diffraction studies of the superstructures in a number of YBCO related cuprate superconductors indicate that the ordering, which is responsible for various type of commensurate or incommensurate superlattices, is mainly confined to the MO_{1-x} "chain" layers; the complementing block of layers remains hardly affected. This supports a simple general concept [11] of the superconducting cuprate crystal structure: the overall structure can be schematised as an alternating stack of pseudo–tetragonal "block"–layers which consists a number of CuO_2 planes (interleaved and/or surrounded by the layers of either perovskite, or rock–salt, or fluorite type structure), and the "non-tetragonal" MO_{1-x}-"chain" layer which determines the overall crystal symmetry.

Acknowledgements

The author is grateful to G. Van Tendeloo, T. Krekels, S. Amelinckx, EMAT Department, University of Antwerp, Belgium, for the fruitful collaboration, and to C. Greaves, School of Chemistry, University of Birmingham, UK, for providing the samples. The work has been financially supported by the Belgian NFWO Foundation and the SU/03/17 Programme. I acknowledges the DG XII of ECC for the grant No. S/CII*913167, and the Croatian Ministry of Science and Technology for supporting my work within the Project 03-057.

References

1) H. Shaked, P. M. Keane, J. C. Rodriguez, F. F. Owen, R. J. Hitterman and J. D. Jorgensen, in *Crystal Structures of the High-T_c Superconducting Copper Oxides*, (Elsvier Sci. B.V., Amsterdam) 1994;

2) S. Adachi, O. Inoue, S. Kawashima, H. Adachi, Y. Ichikawa, K. Setsune and K. Wasa, Physica C **168** (1990) 1;

3) J. G. Bednorz and K. A. Müller, Z. Phys. B **64** (1986) 189;

4) M. K. Wu, R. J. Ashburn, C. J. Torng, P. H. Hor, R. L. Meng, L. Gao, Z. J. Huang, J. Q. Wang and C. W. Chu, Phys. Rev. Lett. **58** (1987) 908;

5) C. Greaves and P. R. Slater, Physica C **161** (1989) 245;

6) C. Greaves, M. Al-Mamouri, P. R. Slater and P. P. Edwards, Physica C **235-240** (1994) 158;

7) Y. Tokura, T. Arima, H. Tagaki, S. Uchida, T. Ishigaki, H. Asano, R. Beyers, A. I. Nazal, P. Lacorre and J. B. Torrance, Nature **342** (1989) 890;

8) S. N. Putilin, E. V. Antipov, O. Chmaissem and M. Marezio, Nature **262** (1993) 226;

9) A. Maignan, M. Hervieu, C. Michel and B. Raveau, Physica C **208** (1993) 116;

10) S. Amelinckx and G. Van Tendeloo, Physica C **235-240** (1994) 162;

11) O. Milat, T. Krekels, G. Van Tendeloo and S. Amelinckx, Physica C **235-240** (1994) 729;

12) G. Van Tendeloo, T. Krekels, O. Milat and S. Amelinckx, J. Alloys and Compounds **195** (1993) 307;

13) G. Roth, P. Adelmann, G. Heger, R. Knitter and Th. Wolf, J. de Physique I **1** (1991) 721;

14) O. Milat, T. Krekels, G. Van Tendeloo and S. Amelinckx, J. de Physique I **3** (1993) 1219;

15) T. Krekels, O. Milat, G. Van Tendeloo, S. Amelinckx, T. G. N. Babu, A. J. Wright and C. Greaves, J. Sol. State Chem. **105** (1993) 313;

16) O. Milat, T. Krekels, G. Van Tendeloo and S. Amelinckx, in *Electron Microscopy 1994* - Proceedings ICEM 13, Paris, vol. 2B, ed. B. Jouffrey and C. Collie (Les Editions de Physique, Les Ulis Cedex A, 1994) pp.859;

17) O. Milat, T. Krekels, S. Amelinckx, T. G. N. Babu and C. Greaves, Physica C **217** (1993) 444;

18) M. Hervieu, G. Van Tendeloo, A. Maignam, C. Michel, F. Goutenoire and B. Raveau, Physica C **216** (1993) 264;

19) P. R. Slater, C. Greaves, M. Slaski and C. M. Muirhead, Physica C **208** (1993) 193;

20) T. Krekels, O. Milat, G. Van Tendeloo, J. Van Landuyt, S. Amelinckx, P. R. Slater and C. Greaves, Physica C **210** (1993) 439;

21) R. J. Cava, A. W. Hewat, E. A. Hewat, B. Batlogg, M. Marezio, K. M. Rabe, J. J. Krajewski, W. F. Peck Jr and L. W. Rupp Jr, Physica C **165** (1989) 419;

22) R. Beyers, B. T. Ahn, G. Gorman, V .Y. Lee, S. S. P. Parkin, M. L. Ramirez, K. P. Roche, J. E. Vasquez, T. M. Gur and R. J. Huggings, Nature **340** (1989) 619.

ELEKTRONSKO MIKROSKOPIJSKO PROUČAVANJE UREĐENJA RAVNINA–"LANACA" KOD VISOKOTEMPERATURNIH SUPRAVODIČA TIPA YBCO

Strukture nekih supravodljivih kuprata, sličnih osnovnom spoju YBCO s visokim T_c, proučavane su tehnikom visoko-razlučujuće elektronske mikroskopije i elektronske difrakcije. Nađeno je da zamjena atoma bakra u ravninama "lanaca" raznim metalnim atomima uzrokuje njihovo uređenje i pojavu sumjerljivih nadstruktura ili nesumjerljivo moduliranih struktura. Odgovarajuće uređenje metalnih (M) i kisikovih (O) atoma ograničeno je na MO_{1-x} ravnine "lanaca" bez većeg utjecaja kako na ostali dio strukture, tako i na osnovna supravodljiva svojstva.